

SCALING GROUP ANALYSIS ON MHD EFFECTS ON HEAT TRANSFER NEAR A STAGNATION POINT ON A LINEARLY STRETCHING SHEET WITH VARIABLE VISCOSITY AND THERMAL CONDUCTIVITY, VISCOUS DISSIPATION AND HEAT SOURCE/SINK

Hunegnaw Dessie and Kishan Naikoti

ABSTRACT. The effects of variable viscosity and thermal conductivity on MHD heat transfer flow of viscous incompressible electrically conducting fluid near stagnation point flow on non-conducting stretching sheet in presence of uniform transfer magnetic field with heat source/sink and viscous dissipation has been analyzed. The governing partial differential equations are transformed into ordinary differential equations using a special form of Lie group transformations and then solved using Fourth order Runge–Kutta Method. Effects of different physical parameters on the flow and heat transfer characteristics are analyzed. Variations of different parameters on skin friction coefficient $f''(0)$ and temperature gradient $-\theta'(0)$ are presented in tabular form.

1. Introduction

The flow due to stretching sheet is a vital problem in classical fluid mechanics due to its applications in many manufacturing processes in industry, such as extraction of polymer sheet, wire drawing, paper production, glass-fiber production, and hot rolling. Crane [1] first investigated the steady boundary layer flow of an incompressible viscous fluid over a linearly stretching plate and gave an exact similarity solution in closed analytical form. Numerous studies [2–10] have been conducted later to extend the pioneering work of Crane [1]. The study of hydrodynamic stagnation point flow over a stretching surface has attracted much attention due to their many practical applications such as MHD generators and cooling of infinite metallic plates in a bath. Hiemenz [11] first studied two-dimensional stagnation flow using similarity transformations to reduce the Navier–Stokes equations to non-linear ordinary differential equations. Ramachandran et al. [12] studied laminar mixed convection in two dimensional stagnation flows around heated surfaces by considering both an arbitrary wall temperature and a varying arbitrary surface

2010 *Mathematics Subject Classification:* 80A20; 76E06; 76D99.

Key words and phrases: scaling group transformation, MHD, stagnation point, variable viscosity and thermal conductivity, heat source/sink, viscous dissipation.

heat flux. Vajravelu and Hadyinicolaou [13] considered convection heat transfer in an electrically conducting fluid near an isothermal stretching sheet and the effect of internal heat generation or absorption. Hiemenz [14] first studied the steady flow in the neighborhood of a stagnation point. Chiam [15] considered a problem which is a combination of the works of Hiemenz [14] and Crane [1] i.e., the stagnation point flow towards a stretching sheet taking identical stretching rate of the sheet and strain rate of the stagnation point flow and he found no boundary layer structure near the sheet. Mahapatra et al. [16] reinvestigated the same stagnation point flow towards a stretching sheet with different stretching and straining rates and found two kinds of boundary layer near the sheet depending on the ratio of the stretching and straining rates. The effects of thermal radiation and viscous dissipation on MHD heat and mass diffusion flow past an oscillating vertical plate embedded in a porous medium with variable surface condition is investigated by Kishore et al. [17] In addition, some very important investigations in this direction can be found in the articles [18–26]. Viscous dissipation changes the temperature distributions by playing a role like an energy source, which leads to affected heat transfer rates. The merit of the effect of viscous dissipation depends on whether the plate is being cooled or heated. Heat transfer analysis over porous surface is of much practical interest due to its abundant applications. All the above mentioned investigations were carried out for fluids having constant viscosity and thermal conductivity throughout the boundary-layer. However it is known that these physical properties may change significantly with temperature. For instance, the viscosity of water decreases about 240% when the temperature increases from 10°C to 50°C. The viscosity of air is 0.6924×10^{-5} , 1.3289, 2.286, and 3.625 at temperatures 1000, 2000, 4000, and 8000 K respectively. To predict accurately the flow behaviors, it is necessary to take the variation of viscosity and thermal conductivity into account. Chamkha [27] discussed the effect of thermal and concentration buoyancy on an unsteady two-dimensional laminar MHD flow which is heat-absorbing over a moving vertical plate. So in order to predict accurately the flow behavior, it is necessary to take into account this variation in viscosity since recent results on the flow due to stretching surface with and without buoyancy force have shown that when this effect is included, the flow characteristics may be substantially changed compared to the constant viscosity case. Pop et al. [28] studied the effect of variable viscosity on flow and heat transfer to a continuous moving flat plate using the similarity solution with no buoyancy force. Mukhopadhyay et al. [29] studied the boundary layer flow over a heated stretching sheet with variable viscosity in the presence of magnetic field. Ali [30] studied the effect of temperature-dependent viscosity on mixed convection heat transfer along a vertical moving surface taking into account the effect of buoyancy force. Mohaimin et al. [31] studied variable viscosity and thermophoresis effects on Darcy mixed convective heat and mass transfer past a porous wedge in the presence of chemical reaction. Abd El-Aziz [32] studied the problem of temperature-dependent viscosity and thermal conductivity effects on combined heat and mass transfer in MHD three-dimensional flow over a stretching surface with Ohmic heating. Salem [33] investigated variable viscosity and thermal conductivity effects on MHD flow heat transfer in visco-elastic fluid over a

stretching sheet. Hassanian et al. [34] investigated the steady non-Darcy mixed convection flow near the stagnation point on a heated vertical surface embedded in a porous medium with thermal radiation and variable viscosity. Sharidan et al. [35] investigated the unsteady flow and heat transfer over a stretching sheet in viscous and incompressible fluid. Pop et al. [36] studied unsteady flow past a stretching sheet. Nazar et al. [37] have studied unsteady boundary layer flow in the region of the stagnation point on a stretching sheet. Seddeek et al. [38] studied the effects of variable viscosity and thermal conductivity on an unsteady two dimensional laminar flow of a viscous incompressible conducting fluid past a semi-infinite vertical porous moving plate taking into account the effect of a magnetic field in the presence of variable suction. Odd et al. [39] have considered the effects of variable viscosity and variable thermal conductivity on heat transfer from a stretching sheet. The effects of MHD and thermal radiation on forced convective flow over a porous plate embedded in porous medium is investigated by Shanmuga [40]. Olajuwon [41] studied heat transfer in a power law with variable thermal conductivity. Hossain et al. [42] considered a steady two-dimensional laminar forced flow and heat transfer of a viscous incompressible fluid having temperature dependent viscosity and thermal conductivity past a wedge with a uniform surface heat flux. In formulating the equations governing the flow both the viscosity and the thermal conductivity of the fluid are considered to be linear function of temperature. In the field of fluid mechanics, most of the researchers try to obtain the similarity solutions in such cases using the similarity variables. In case of scaling group of transformations, the group-invariant solutions are nothing but the well known similarity transformation (Boutros Y. Z et al. [43]). A special form of Lie-group of transformations known as scaling is used in this paper to find out the full set of symmetries of the problem and then to study which of them are appropriate to provide group invariant or more specifically similarity solutions. This method reduces the system of non-linear coupled partial differential equations governing the motion of the fluid into a system of coupled non-linear ordinary differential equations. In this paper, by applying Lie's scaling group transformations to the problem of boundary layer flow and heat transfer of a fluid with variable viscosity and variable thermal conductivity near a stagnation point on a linearly stretching sheet by taking the effects of viscous dissipation and heat source/sink in the presence of uniform magnetic field is analyzed. The system remains invariant due to some relations among the parameters of the transformations. With this transformation, a third order and a second order ordinary differential equations corresponding to momentum and energy equations are derived. These equations are solved with the help of Runge–Kutta fourth order method along with shooting technique. The effects of the fluid viscosity parameter, Prandtl number, magnetic parameter, velocity ratio parameter, thermal conductivity, variable viscosity parameter, Eckert parameter and heat source/sink parameter on velocity and temperature fields are investigated and analyzed with the help of graphical representation.

2. Formulation of the problem

Consider the steady MHD boundary layer flow of a viscous incompressible electrically conducting fluid of variable viscosity and variable thermal conductivity in the vicinity of a stagnation point on a non-conducting stretching sheet in the presence of heat generation/absorption and viscous dissipation. The stretching sheet has uniform temperature T_w , linear velocity $u_w(x)$. It is assumed that all external force fields except magnetic field are zero. The stretching sheet coincides with plane $y = 0$ and the flow is confined in the region $y > 0$. The x and y axes are taken along and perpendicular to the sheet, respectively. Uniform magnetic field of strength B_0 is imposed along the y -axis.

The governing equations of motion for the steady two dimensional flow under the influence of externally imposed transverse magnetic field with variable thermal conductivity and variable viscosity in the boundary layer are

$$\begin{aligned} & \frac{\partial u}{\partial x} + \frac{\partial v}{\partial y} = 0 \\ (2.1) \quad & u \frac{\partial u}{\partial x} + v \frac{\partial u}{\partial y} = -\frac{1}{\rho} \frac{\partial p}{\partial x} + \frac{1}{\rho} \frac{\partial}{\partial y} \left(\mu \frac{\partial u}{\partial y} \right) - \frac{\sigma B_0^2}{\rho} u \end{aligned}$$

$$(2.2) \quad u \frac{\partial T}{\partial x} + v \frac{\partial T}{\partial y} = \frac{\alpha}{\rho c_p} \frac{\partial}{\partial y} \left(k^* \frac{\partial T}{\partial y} \right) + \frac{\mu}{\rho c_p} \left(\frac{\partial u}{\partial y} \right)^2 + \frac{Q_0}{\rho c_p} (T - T_\infty)$$

where u and v are components of velocity respectively in x and y directions, $\nu = \frac{\mu}{\rho}$, T is the temperature, T_∞ is the free stream temperature is the fluid the thermal conductivity, Q_0 is the volumetric heat generation ($Q_0 > 0$) or absorption ($Q_0 < 0$) coefficient, c_p is the specific heat, ρ is the fluid density (assumed constant), μ is the fluid viscosity. In the free stream $u = U(x) = bx$, the equation (2.1) reduces to

$$(2.3) \quad U \frac{dU}{dx} = -\frac{1}{\rho} \frac{\partial p}{\partial x} - \frac{\sigma B_0^2}{\rho} U$$

Eliminating $\frac{\partial p}{\partial x}$ between the equations (2.1) and (2.3), we obtain

$$u \frac{\partial u}{\partial x} + v \frac{\partial u}{\partial y} = U \frac{dU}{dx} + \frac{1}{\rho} \frac{\partial}{\partial y} \left(\mu \frac{\partial u}{\partial y} \right) - \frac{\sigma B_0^2}{\rho} (u - U)$$

2.1. Boundary conditions. The boundary conditions for the problem are given by

$$\begin{aligned} u &= u_w(x) = cx, & v &= 0, & T &= T_w \text{ at } y = 0, \\ u &= U(x) = bx, & & & T &= T_\infty \text{ at } y \rightarrow \infty \end{aligned}$$

Here $c > 0$ is the stretching constant, T_w is the uniform wall temperature, T_∞ is the temperature far away from the sheet. Following Ling et al. [44] and Lai and kulacki et al. [45], we take the temperature-dependent viscosity of the form

$$(2.4) \quad \mu = \frac{\mu_\infty}{[1 + a(T - T_\infty)]}$$

where μ_∞ is a constant value of the coefficient of viscosity far away from the sheet and $a > 0$ is a constant. Note that the dimensionless temperature θ can also be

written as

$$(2.5) \quad \theta = \frac{T - T_r}{T_w - T_\infty} + \theta_r, \quad \theta_r = \frac{T_r - T_\infty}{T_w - T_\infty}, \quad T_r = T_\infty - \frac{1}{a}$$

Substituting (2.5) into (2.4), we immediately find

$$\mu = \mu_\infty \frac{\theta_r}{\theta_r - \theta}$$

The variation of the thermal conductivity k^* is taken of form as

$$k^* = k_\infty (1 + \varepsilon\theta)$$

where k_∞ is the value of the thermal diffusivity at the surface of temperature T_w and ε is a parameter that depends on the nature of the fluid.

2.2. Method of Solution. Introducing the following relations for u, v, θ as

$$u = \frac{\partial\psi}{\partial y}, \quad v = -\frac{\partial\psi}{\partial x}, \quad \theta = \frac{T - T_\infty}{T_w - T_\infty}$$

where ψ is the stream function.

Using the relations (2.5) in the boundary layer equation (2.1) and in the energy equation (2.2) we get the following equations

$$(2.6) \quad \frac{\partial\psi}{\partial y} \frac{\partial^2\psi}{\partial x\partial y} - \frac{\partial\psi}{\partial x} \frac{\partial^2\psi}{\partial y^2} = U \frac{dU}{dx} + \frac{\mu_\infty}{\rho_\infty} \frac{\theta_r}{(\theta_r - \theta)^2} \frac{\partial\theta}{\partial y} \frac{\partial^2\psi}{\partial y^2} \\ + \frac{\mu_\infty}{\rho_\infty} \frac{\theta_r}{\theta_r - \theta} \frac{\partial^3\psi}{\partial y^3} - \frac{\sigma B_0^2}{\rho_\infty} \left(\frac{\partial\psi}{\partial y} - U \right)$$

$$(2.7) \quad \frac{\partial\psi}{\partial y} \frac{\partial\theta}{\partial x} - \frac{\partial\psi}{\partial x} \frac{\partial\theta}{\partial y} = \frac{k_\infty\varepsilon}{\rho_\infty C_p} \left(\frac{\partial\theta}{\partial y} \right)^2 + \frac{k_\infty}{\rho_\infty C_p} (1 + \varepsilon\theta) \frac{\partial^2\theta}{\partial y^2} + \frac{Q_0}{\rho_\infty C_p} \theta \\ + \frac{1}{\rho_\infty C_p (T_w - T_\infty)} \frac{\theta_r}{\theta_r - \theta} \left(\frac{\partial^2\psi}{\partial y^2} \right)^2$$

The boundary conditions (2.3) then becomes

$$(2.8) \quad \frac{\partial\psi}{\partial y} = cx, \quad \frac{\partial\psi}{\partial x} = 0, \quad \theta = 1 \text{ as } y = 0 \\ \frac{\partial\psi}{\partial y} = U(x) = bx, \quad \theta = 0 \text{ as } y \rightarrow \infty.$$

2.3. Scaling group of transformations. Now introduce simplified form of Lie-group transformations namely the scaling group of transformations (Mukhopadhyay et al. [29] and Dessie et al. [46]),

$$(2.9) \quad \Gamma : x^* = xe^{\varepsilon\alpha_1}, \quad y^* = ye^{\varepsilon\alpha_2}, \quad \psi^* = \psi e^{\varepsilon\alpha_3}, \quad u^* = ue^{\varepsilon\alpha_4} \\ v^* = ve^{\varepsilon\alpha_5}, \quad U^* = Ue^{\varepsilon\alpha_6}, \quad \theta^* = \theta e^{\varepsilon\alpha_7}$$

Equation (2.9) may be considered as a point-transformation which transforms coordinates $(x, y, \psi, u, v, \theta)$ to the coordinates $(x^*, y^*, \psi^*, u^*, v^*, \theta^*)$. Substituting (2.9) in (2.6) and (2.7), we get,

$$\begin{aligned}
(2.10) \quad & e^{\varepsilon(\alpha_1+2\alpha_2-2\alpha_3)} \left(\frac{\partial\psi^*}{\partial y^*} \frac{\partial^2\psi^*}{\partial x^* \partial y^*} - \frac{\partial\psi^*}{\partial x^*} \frac{\partial^2\psi^*}{\partial y^{*2}} \right) \left(1 - \frac{\theta^* e^{-\varepsilon\alpha_7}}{\theta_r} \right)^2 \\
& = e^{\varepsilon(\alpha_1-2\alpha_6)} U^* \frac{dU^*}{dx^*} \left(1 - \frac{\theta^* e^{-\varepsilon\alpha_7}}{\theta_r} \right)^2 \\
& \quad + \frac{v_\infty}{\theta_r} e^{\varepsilon(3\alpha_2-\alpha_3-\alpha_7)} \frac{\partial\theta^*}{\partial y^*} \frac{\partial^2\psi^*}{\partial y^{*2}} \\
& \quad + v_\infty \left(1 - \frac{\theta^* e^{-\varepsilon\alpha_7}}{\theta_r} \right) e^{\varepsilon(3\alpha_2-\alpha_3)} \frac{\partial^3\psi^*}{\partial y^{*3}} \\
& \quad - \frac{\sigma B_0^2}{\rho_\infty} e^{\varepsilon(\alpha_2-\alpha_3)} \left(\frac{\partial\psi^*}{\partial y^*} - U^* e^{-\varepsilon\alpha_6} \right) \left(1 - \frac{\theta^* e^{-\varepsilon\alpha_7}}{\theta_r} \right)^2
\end{aligned}$$

$$\begin{aligned}
(2.11) \quad & e^{\varepsilon(\alpha_1+\alpha_2-\alpha_3-\alpha_7)} \left(\frac{\partial\psi^*}{\partial y^*} \frac{\partial\theta^*}{\partial x^*} - \frac{\partial\psi^*}{\partial x^*} \frac{\partial\theta^*}{\partial y^*} \right) \left(1 - \frac{\theta^* e^{-\varepsilon\alpha_7}}{\theta_r} \right) \\
& = \frac{k}{\rho C_p} e^{\varepsilon(2\alpha_2-2\alpha_7)} \left(\frac{\partial\theta^*}{\partial y^*} \right)^2 \left(1 - \frac{\theta^* e^{-\varepsilon\alpha_7}}{\theta_r} \right) \\
& \quad + \frac{k_\infty}{\rho_\infty c_p} (1 + \varepsilon\theta^* e^{-\varepsilon\alpha_7}) e^{\varepsilon(2\alpha_2-\alpha_7)} \frac{\partial^2\theta^*}{\partial y^{*2}} \left(1 - \frac{\theta^* e^{-\varepsilon\alpha_7}}{\theta_r} \right) \\
& \quad + \frac{Q_0}{\rho_\infty c_p} \theta^* e^{-\varepsilon\alpha_7} \left(1 - \frac{\theta^* e^{-\varepsilon\alpha_7}}{\theta_r} \right) \\
& \quad + \frac{1}{\rho_\infty c_p (T_w - T_\infty)} e^{\varepsilon(4\alpha_2-2\alpha_3)} \left(\frac{\partial^2\psi^*}{\partial y^{*2}} \right)^2
\end{aligned}$$

The system will remain invariant under the group of transformations Γ we would have the following relations among the parameters, namely

$$\begin{aligned}
\alpha_1 + 2\alpha_2 - 2\alpha_3 &= \alpha_1 - 2\alpha_2 - 2\alpha_3 - \alpha_7 = \alpha_1 + 2\alpha_2 - 2\alpha_3 - 2\alpha_7 = \alpha_1 - 2\alpha_6 \\
&= \alpha_1 - 2\alpha_6 - \alpha_7 = \alpha_1 - 2\alpha_6 - 2\alpha_7 = 3\alpha_2 - \alpha_3 - \alpha_7 \\
&= 3\alpha_2 - \alpha_3 = \alpha_2 - \alpha_3 = -\alpha_6 = \alpha_2 - \alpha_3 - \alpha_7 \\
&= -\alpha_6 - \alpha_7\alpha_2 - \alpha_3 - 2\alpha_7 = -\alpha_6 - 2\alpha_7
\end{aligned}$$

and

$$\begin{aligned}
\alpha_1 + \alpha_2 - \alpha_3 - \alpha_7 &= \alpha_1 + \alpha_2 - \alpha_3 - 2\alpha_7 = 2\alpha_2 - 2\alpha_7 = 2\alpha_2 - 3\alpha_7 \\
&= 2\alpha_2 - \alpha_7 = -\alpha_7 = -2\alpha_7 = 4\alpha_2 - 2\alpha_3
\end{aligned}$$

Taking account into the boundary conditions and the above relations gives $\alpha_1 = \alpha_3 = \alpha_4 = \alpha_6$ and $\alpha_2 = \alpha_5 = \alpha_7 = 0$. Thus the set reduces to a one parameter group of transformations:

$$\begin{aligned}
(2.12) \quad & x^* = x e^{\varepsilon\alpha_1}, \quad y^* = y, \quad u^* = u e^{\varepsilon\alpha_1}, \\
& v^* = v, \quad U^* = U e^{\varepsilon\alpha_1}, \quad \psi^* = \psi e^{\varepsilon\alpha_1}, \quad \theta^* = \theta
\end{aligned}$$

Expanding by Taylor's series we get

$$\begin{aligned}
(2.13) \quad & x^* - x = x\varepsilon\alpha_1, \quad y^* - y = 0, \\
& u^* - u = u\varepsilon\alpha_1, \quad \psi^* - \psi = \psi\varepsilon\alpha_1
\end{aligned}$$

$$v^* - v = 0, \quad U^* - U = U\varepsilon\alpha_1, \quad \theta^* - \theta = 0$$

The characteristic equations are

$$(2.14a) \quad \frac{dx}{\alpha_1 x} = \frac{dy}{0} = \frac{d\psi}{\alpha_1 \psi} = \frac{dU}{\alpha_1 U} = \frac{du}{\alpha_1 u} = \frac{dv}{0} = \frac{d\theta}{0}$$

From the subsidiary equations $\frac{dx}{\alpha_1 x} = \frac{dy}{0}$ we get $dy = 0$ which on integrations gives

$$(2.14b) \quad y = \eta \quad (\text{constant}) \quad (\text{say})$$

From equations $\frac{dx}{\alpha_1 x} = \frac{d\theta}{0}$ we get $d\theta = 0$ which on integration gives us

$$(2.14c) \quad \theta = \theta(\eta) \quad (\text{say})$$

Also integrating the equations $\frac{dx}{\alpha_1 x} = \frac{d\psi}{\alpha_1 \psi}$ we get $\frac{\psi}{x} = \text{constant}$

$$(2.14d) \quad \psi = xF(\eta) \quad (\text{say})$$

where F is an arbitrary function of η .

Thus from equations (2.14b)–(2.14d) we obtain,

$$y = \eta, \quad \psi = xF(\eta), \quad \theta = \theta(\eta)$$

Using these transformation equations (2.10) and (2.11) becomes

$$(2.15) \quad v_\infty F''' - \left(F'^2 - FF'' - b^2 - \frac{\sigma B_0^2}{\rho} (F' - b) \right) \left(1 - \frac{\theta}{\theta_r} \right) = 0$$

$$(2.16) \quad \frac{k_\infty}{\rho_\infty C_p} (1 + \varepsilon\theta)\theta'' \left(1 - \frac{\theta}{\theta_r} \right) + \frac{k}{\rho C_p} \varepsilon\theta'^2 \left(1 - \frac{\theta}{\theta_r} \right) + F\theta' \left(1 - \frac{\theta}{\theta_r} \right) \\ + \frac{Q_0}{\rho_\infty c_p} \theta \left(1 - \frac{\theta}{\theta_r} \right) + \frac{\mu_\infty x^2}{\rho_\infty c_p (T_w - T_\infty)} F''^2 = 0$$

The boundary conditions of equation (2.8) becomes

$$F' = c, \quad F = 0, \quad \theta = 1, \quad \text{at } \eta = 0 \\ F' = b, \quad \theta = 0 \quad \text{at } \eta \rightarrow \infty$$

Introducing $\eta = v^\alpha c^\beta \eta^*$, $F = v^{\alpha'} c^{\beta'} F^*$, $\theta = v^{\alpha''} c^{\beta''} \bar{\theta}$ in equations (2.15) and (2.16) we get $\alpha' = \alpha = 1/2$, $\alpha'' = 0$, $\beta = -1/2$, $\beta' = 1/2$, $\beta'' = 0$. The equations (2.15) and (2.16) are transformed to

$$(2.17) \quad F^{*'''} - (F^{*'}{}^2 - F^* F^{*''} - \lambda^2 + M(F^{*'} - \lambda)) \left(1 - \frac{\bar{\theta}}{\theta_r} \right) = 0$$

$$(2.18) \quad (1 + \varepsilon\bar{\theta})\bar{\theta}'' + \varepsilon\bar{\theta}'^2 + \text{Pr}(F^* \bar{\theta}' + h\bar{\theta}) + \text{Pr Ec} \left(1 - \frac{\bar{\theta}}{\theta_r} \right) F^{*''2} = 0$$

where $\text{Pr} = \left(1 - \frac{\bar{\theta}}{\theta_r} \right)^{-1} \text{Pr}_\infty$ where $\text{Pr}_\infty = \frac{\mu_\infty c_p}{k_\infty}$ is the Prandtl number and $S = \frac{Q_0}{c_p c_p}$ is the heat source/sink parameter, $\lambda = \frac{b}{c}$ is velocity ratio parameter, $M = \frac{\sigma B_0^2}{\rho c}$ is the magnetic parameter, $\text{Ec} = \frac{c^2 x^2}{c_p (T_w - T_\infty)}$ is Eckert number.

Taking $F^* = f$ and $\bar{\theta} = \theta$ the equations (2.17) and (2.18) finally takes the following form

$$(2.19) \quad f''' - (f'^2 - f f'' - \lambda^2 + M(f' - \lambda)) \left(1 - \frac{\theta}{\theta_r}\right) = 0$$

$$(2.20) \quad (1 + \varepsilon\theta)\theta'' + \varepsilon\theta'^2 + \text{Pr} \left(f\theta' + h\theta + \text{Ec} \left(1 - \frac{\theta}{\theta_r}\right) f''^2 \right) = 0$$

The boundary conditions (2.13) also reduces

$$(2.21) \quad \begin{aligned} f' &= 1, & f &= 0, & \theta &= 1 & \text{at } \eta = 0 \\ f' &= \lambda = \frac{b}{c}, & \theta &= 0 & & & \text{as } \eta \rightarrow \infty \end{aligned}$$

3. Numerical Method for Solution

The set of coupled non-linear governing boundary layer equations (2.19) and (2.20) together with boundary conditions equations (2.21) are solved numerically by using Runge–Kutta fourth order technique along with shooting method. First of all, the higher order non-linear differential equations (2.19) and (2.20) are converted into simultaneous linear differential equation of first order and they are further transformed into initial value problem by applying the shooting technique. Once the problem is reduced to initial value problem, then it is solved by Runge-Kutta fourth order technique.

Skin-friction. Skin-friction coefficient at the sheet is given by

$$C_f = \frac{\tau_w}{\rho(c\nu)^{1/2}} = x f''(0) \text{ where } \tau_w = \mu \left(\frac{\partial u}{\partial y} + \frac{\partial v}{\partial x} \right)_{y=0}$$

is the shear stress at the sheet.

Nusselt number. The rate of heat transfer in terms of the Nusselt number at the sheet is given by

$$Nu = \left(\frac{v}{c} \right)^{1/2} \frac{q_w}{k^*(T_w - T_\infty)} = -\theta'(0) \text{ where } q_w = -k^* \left(\frac{\partial T}{\partial y} \right)_{y=0}$$

4. Results and Discussion

The set of non-linear ordinary differential equations (2.19) and (2.20) with boundary conditions of equations (2.21) have been solved by using the fourth-order Runge–Kutta method with systematic estimates of $f''(0)$ and $-\theta'(0)$ by the shooting technique. In this calculation the step size $\Delta(\eta) = 0.001$ and six decimal accuracy as the criterion for convergence are used. In order to verify the validity and accuracy of the present results, the values for the skin-friction $f''(0)$ and heat transfer rate $-\theta'(0)$ were compared with those reported by Pop and Grosan (2004) and Mahapara and Gupta (2009). The comparison in the above cases is found to be in excellent agreement as shown in the Table 1 and Table 2. The values of Local skin-friction coefficient and temperature gradient are tabulated in Table 3 and Table 4. It is noted that from Table 3, both the values of the skin-friction coefficient $f''(0)$ and local Nusselt number $-\theta'(0)$ decrease with increasing of heat source/sink parameter S.

TABLE 1. Values of $f''(0)$ for different values of λ are compared with the results obtained by Pop, Grosan and Pop (2004), Sharma P R and Sighh (2009)

λ	Pop, Grosan & Pop (2004)	$f''(0)$	
		Sharma P. R. & Sighh (2009)	Present paper
0.1	-0.9694	-0.969386	-0.969386
0.2	-0.9181	-0.9181069	-0.918107
0.5	-0.6673	-0.667263	-0.667363
2.0	2.0174	2.01749079	2.017504
3.0	4.7290	4.72922695	4.729282

TABLE 2. Values of $-\theta'(0)$ for different values of λ are compared with the results obtained by Pop, Grosan and Pop (2004) and Sharma P. R. and Sighh (2009).

λ	Pop, Grosan & Pop (2004)	$-\theta'(0)$	
		Sharma P.R and Sighh(2009)	Present paper
0.1	0.081	0.0811245	0.080865
0.2	0.135	0.135571	0.135639
2.0	0.241	0.241025	0.248040

It is also pointed out from Table 3, as the velocity ratio parameter λ increases the skin-friction coefficient $f''(0)$ decreases whereas temperature gradient $-\theta'(0)$ increases. From the same table it can be observed that the increase of thermal conductivity parameter ε is to decrease the value of the skin-friction coefficient $f''(0)$ and the temperature gradient $-\theta'(0)$. When the magnetic parameter value M increases skin-friction coefficient $f''(0)$ increases but temperature gradient $-\theta'(0)$ decreases. From Table 4, it can be seen that when the Eckert number Ec increases both the skin-friction coefficient $f''(0)$ and the temperature gradient $-\theta'(0)$ decrease. It is observed that, the increase of variable viscosity θ_r is to increase the skin-friction coefficient $f''(0)$ and to decrease temperature gradient $-\theta'(0)$. The effects of Prandtl number is to increase both the local skin-friction coefficient $f''(0)$ and temperature gradient $-\theta'(0)$ as it can be seen from Table 3 and Table 4.

The dimensionless velocity and temperature profiles are shown graphically in Figures 1 to 7 for different flow parameters such as velocity ratio λ , thermal conductivity ε , magnetic parameter M , heat source/sink parameter S , Eckert number Ec , Prandtl number Pr and variable viscosity parameter θ_r . Figure 1a shows that the boundary layer thickness decreases considerably as λ increases.

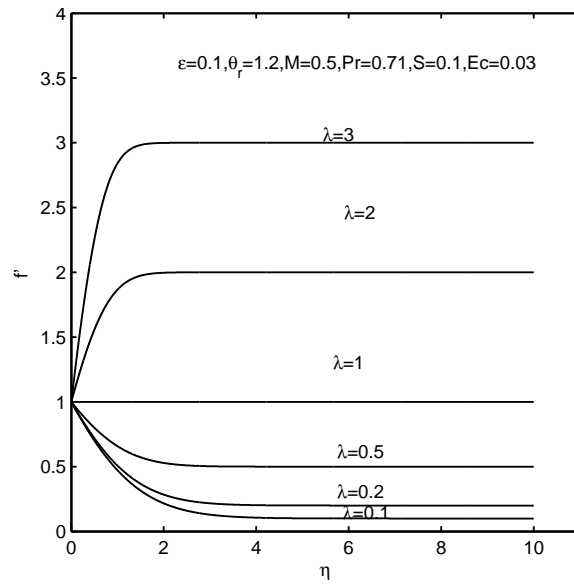
TABLE 3. Values of skin-friction and rate of heat transfer for different values of $M, \lambda, \varepsilon, S, Pr$ for $Ec = 0.03$ and $\theta_r = 1.2$

		$\varepsilon = 0$ and $S = 0$				$\varepsilon = 0$ and $S = 0.1$				$\varepsilon = 0$ and $S = -0.3$			
		$-f''(0)$		$-\theta'(0)$		$f''(0)$		$-\theta'(0)$		$-f''(0)$		$-\theta'(0)$	
M	λ	Pr=0.5	Pr=0.71	Pr=0.5	Pr=0.71	Pr=0.5	Pr=0.71	Pr=0.5	Pr=0.71	Pr=0.5	Pr=0.71	Pr=0.5	Pr=0.71
0.0	0.1	0.60875	0.63385	0.41729	0.51665	0.59475	0.62109	0.35129	0.44273	0.63739	0.66076	.57283	.69076
0.5	0.1	0.65241	0.67925	0.40939	0.50743	0.63651	0.66460	0.34150	0.43144	0.68454	0.70975	.56769	.68874
0	0.5	0.41791	0.43343	0.48745	0.58896	0.41212	0.42775	0.43810	0.53115	0.43182	0.44715	.61634	.74052
0.5	0.5	0.43810	0.45424	0.48546	0.58656	0.43194	0.44816	0.43589	0.52848	0.45287	0.46888	.61479	.73867
		$\varepsilon = 0.1$ and $S = 0$				$\varepsilon = 0.1$ and $S = 0.1$				$\varepsilon = 0.1$ and $S = -.3$			
		$-f''(0)$		$-\theta'(0)$		$-f''(0)$		$-\theta'(0)$		$-f''(0)$		$-\theta'(0)$	
M	λ	Pr=0.5	Pr=0.71	Pr=0.5	Pr=0.71	Pr=0.5	Pr=0.71	Pr=0.5	Pr=0.71	Pr=0.5	Pr=0.71	Pr=0.5	Pr=0.71
0.0	0.1	.60286	.62792	.38948	.48243	0.58882	.61508	0.32719	.41269	.63161	.65501	.53606	.65029
0.5	0.1	.64601	.67273	.38204	.47376	.63010	.65803	.31799	.40208	.67821	.70338	.53125	.64461
0	0.5	.41397	.42944	.45624	.55128	.40818	.42374	.40983	.49692	.42787	.44317	.57742	.69379
0.5	0.5	.43395	.45001	.45437	.54904	.42781	.44393	.40775	.49443	.44869	.46466	.57598	.69205
		$\varepsilon = 0.5$ and $S = 0$				$\varepsilon = 0.5$ and $S = 0.1$				$\varepsilon = 0.5$ and $S = -.3$			
		$-f''(0)$		$-\theta'(0)$		$-f''(0)$		$-\theta'(0)$		$-f''(0)$		$-\theta'(0)$	
M	λ	Pr=0.5	Pr=0.71	Pr=0.5	Pr=0.71	Pr=0.5	Pr=0.71	Pr=0.5	Pr=0.71	Pr=0.5	Pr=0.71	Pr=0.5	Pr=0.71
0.0	0.1	.58329	.60798	.31229	.38750	.56913	.59489	.26025	.32925	.61233	.63561	.43423	.52708
0.5	0.1	.62496	.65102	.30620	.38035	.60903	.63614	.25267	.32046	.65722	.68205	.43030	.52242
0	0.5	.40100	.41614	.36989	.44708	.39528	.41045	.33162	.40223	.41479	.42990	.46978	.56452
0.5	0.5	.42037	.43600	.36837	.44525	.41433	.42996	.32993	.40020	.43492	.45061	.46860	.56312

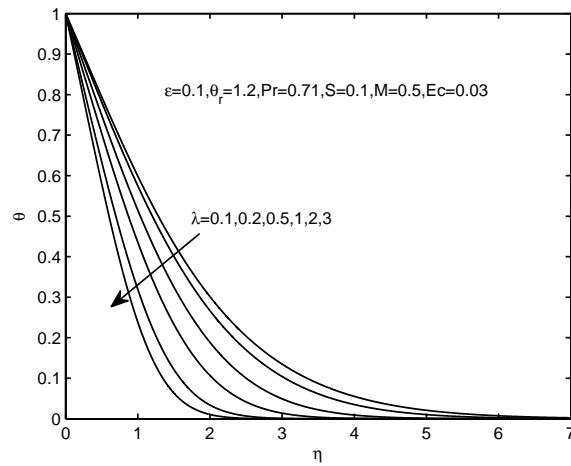
TABLE 4. Values of skin-friction and rate of heat transfer for different values of $M, \lambda, Pr, \theta_r, Ec$ for $\varepsilon = 0, S = 0$

		$M = 0$ and $\lambda = 0.1$				$M = 0$ and $\lambda = 0.5$				$M = 0$ and $\lambda = 2$			
		$-f''(0)$		$-\theta'(0)$		$-f''(0)$		$-\theta'(0)$		$f''(0)$		$-\theta'(0)$	
Ec	θ_r	Pr=0.5	0.71	Pr=0.5	0.71	Pr=0.5	0.71	Pr=0.5	0.71	Pr=0.5	0.71	Pr=0.5	0.71
0.03	1.2	.60874	.63386	.41730	.51664	.41791	.43343	.48745	.58896	1.25898	1.30002	.68932	.81006
0.1	1.2	.60811	.63298	.41385	.51132	.41777	.43324	.48613	.58693	1.25717	1.29755	.68136	.79808
0.03	1.5	.68736	.70586	.40865	.50792	.47273	.48406	.48363	.58491	1.42732	1.45709	.69241	.81294
0.1	1.5	.68678	.70509	.40373	.50059	.47260	.48388	.48171	.58207	1.42564	1.45481	.68073	.79589
		$M = 0.5$ and $\lambda = 0.1$				$M = 0.5$ and $\lambda = 0.5$				$M = 0.5$ and $\lambda = 2$			
		$-f''(0)$		$-\theta'(0)$		$-f''(0)$		$-\theta'(0)$		$f''(0)$		$-\theta'(0)$	
Ec	θ_r	Pr=0.5	0.71	Pr=0.5	0.71	Pr=0.5	0.71	Pr=0.5	0.71	Pr=0.5	0.71	Pr=0.5	0.71
0.03	1.2	.65241	.67925	.40939	.50744	.43810	.45424	.48546	.58656	1.28656	1.32831	.69032	.81128
0.1	1.2	.65170	.67827	.40583	.50191	.43794	.45403	.48410	.58449	1.28470	1.32576	.68227	.79916
0.03	1.5	.74388	.76338	.39969	.49752	.49875	.51043	.48142	.58226	1.46280	1.49294	.69346	.81420
0.1	1.5	.74323	.76250	.39449	.48976	.49861	.51023	.47942	.57931	1.46108	1.49062	.68158	.79685
		$M = 1$ and $\lambda = 0.1$				$M = 1$ and $\lambda = 0.5$				$M = 1$ and $\lambda = 2$			
		$-f''(0)$		$-\theta'(0)$		$-f''(0)$		$-\theta'(0)$		$f''(0)$		$-\theta'(0)$	
Ec	θ_r	Pr=0.5	0.71	Pr=0.5	0.71	Pr=0.5	0.71	Pr=0.5	0.71	Pr=0.5	0.71	Pr=0.5	0.71
0.03	1.2	.76373	.79383	.39231	.48600	.49227	.50991	.48051	.58053	1.36504	1.40871	.69308	.81461
0.1	1.2	.76285	.79263	.38845	.48008	.49209	.50966	.47908	.57831	1.36304	1.40597	.68476	.80209
0.03	1.5	.88944	.91048	.38053	.47332	.56896	.58141	.47599	.57561	1.56388	1.59506	.69629	.81762
0.1	1.5	.88862	.90933	.37459	.46435	.56879	.58119	.47380	.57237	1.56203	1.59255	.68385	.79942

The increase in the value of λ implies that free stream velocity increases in comparison to stretching velocity, which results in the increase in pressure and straining motion near stagnation point and hence thinning of boundary layer takes place.

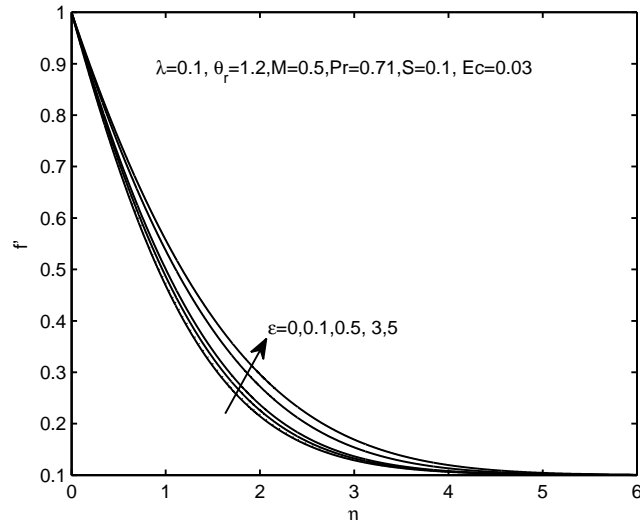


(A)

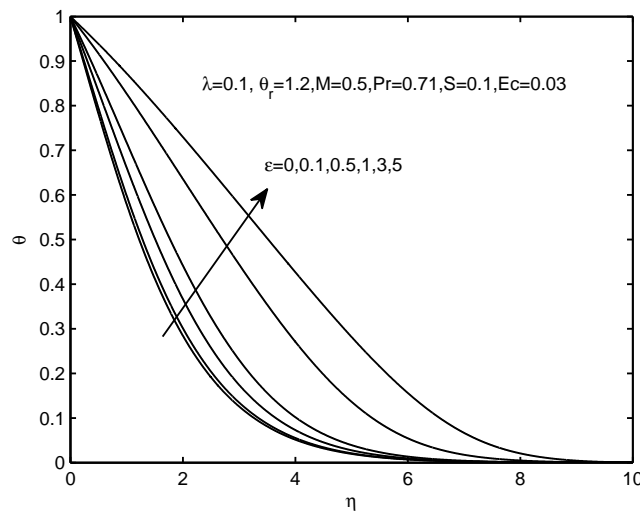


(B)

FIGURE 1. Velocity and temperature profiles for different values of velocity ratio parameter λ



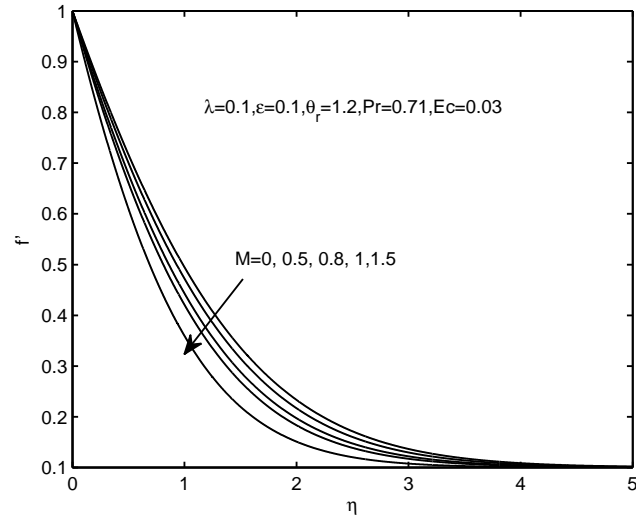
(A)



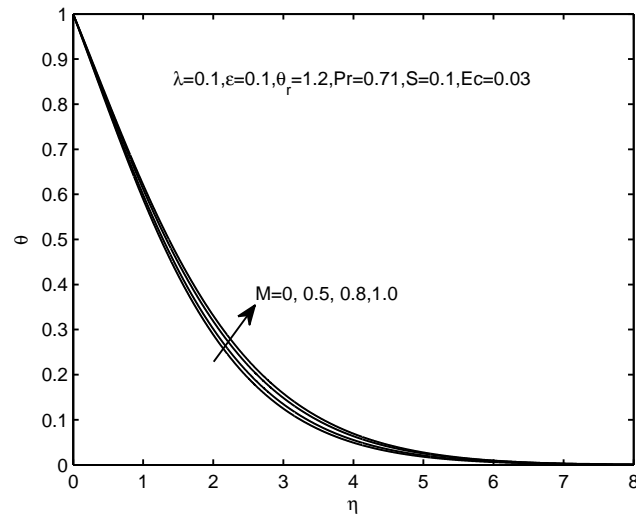
(B)

FIGURE 2. velocity and temperature profiles for different values of thermal conductivity parameter ε

The phenomenon of thinning boundary layer thus implies increased shear stress at the sheet. It is important to note for $\lambda = 1$, that there is no formation of boundary layer because the sheet velocity is equal to free stream velocity. It is seen from Figure 1b that the fluid temperature decreases due to increase of velocity ratio λ . Figures 2a and 2b display the effects of thermal conductivity parameter



(A)



(B)

FIGURE 3. velocity and temperature profiles for different values of magnetic parameter M

ε on the velocity and temperature profiles respectively. Figure 2a shows with the increase in the values of ε velocity profiles f' increases. Fluid temperature θ is also found to increase with increasing values of ε which leads to a fall in the rate of heat transfer from the flow to the surface. Therefore, the rate of cooling is much faster

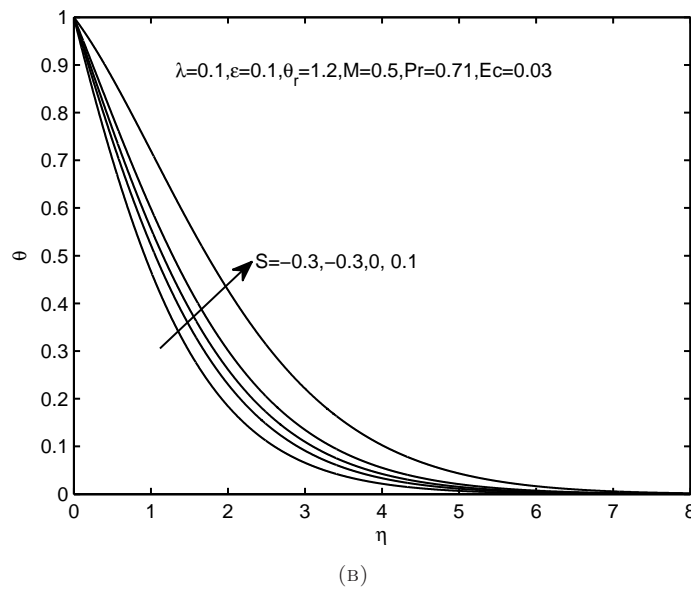
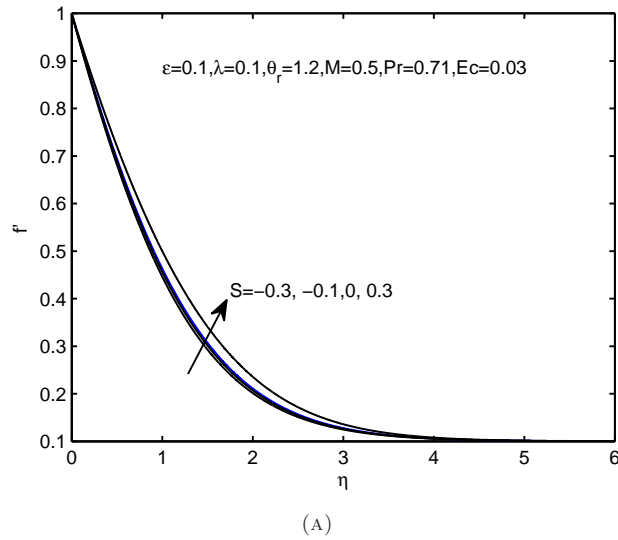


FIGURE 4. velocity and temperature profiles for different values of heat source/sink parameter S

to the coolant material having small thermal conducting parameter. The effect of transverse magnetic field on the velocity field and on temperature profiles are depicted in Figures 3a and 3b respectively. From Figure 3b it is noticed that the rate of transport is considerably reduced with the increase of M . It clearly indicates

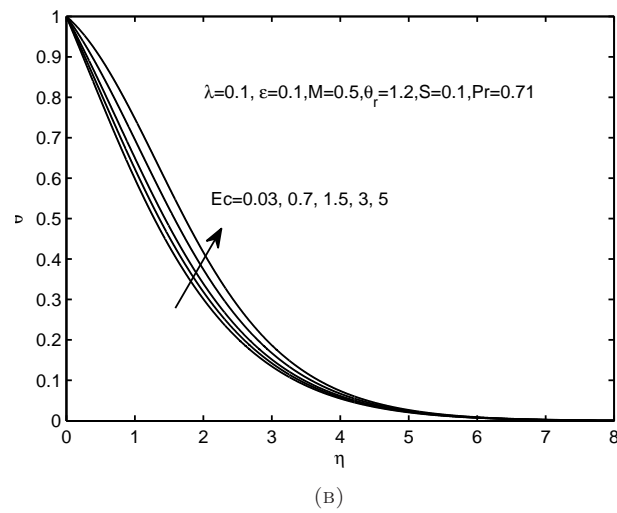
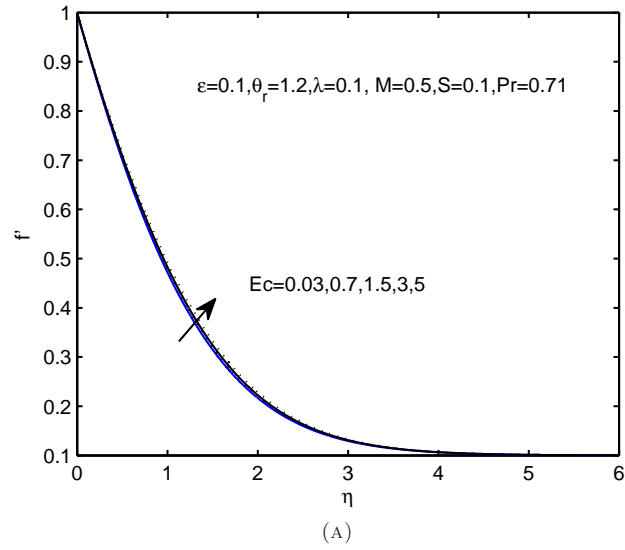


FIGURE 5. velocity and temperature profiles for different values of heat Eckert number Ec

that the transverse magnetic field opposes the transport phenomena. This is due to the fact that the variation of the magnetic number leads to the variation of the Lorentz force due to magnetic field and the Lorentz force produces more resistance to the transport phenomena. In all cases the velocity vanishes at some stage large distance from the sheet. The velocity decreases with increase of magnetic parameter M . From the plots in Figure 3b, it is observed that the transverse magnetic field

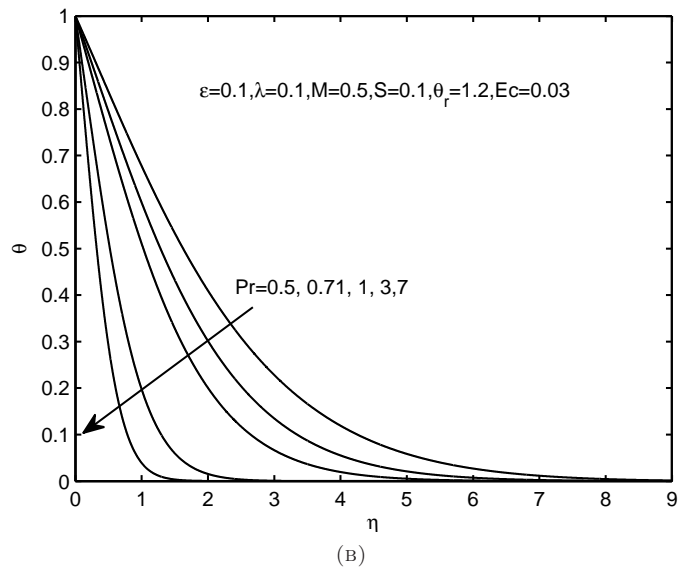
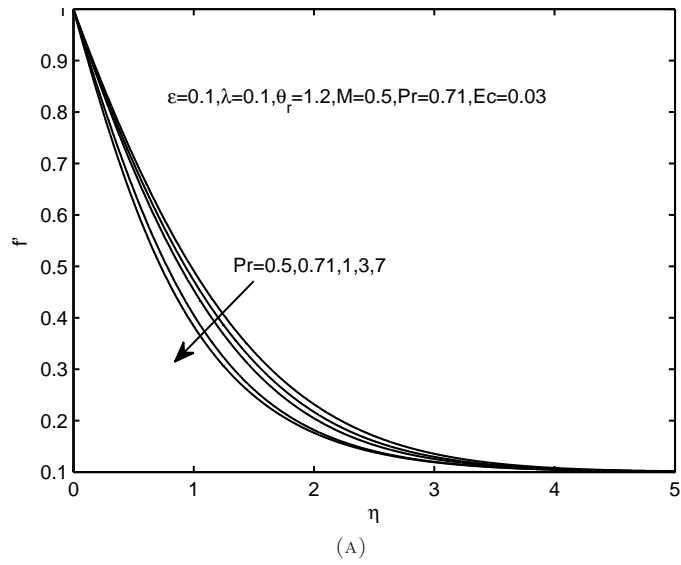


FIGURE 6. velocity and temperature profiles for different values of Prandtl number Pr

contributes to the thickening of the thermal boundary layer. This is evident from the fact that the applied transverse magnetic field produces a body force, to be precise the Lorentz force, which opposes the motion. The resistance offered to the flow is responsible in enhancing the temperature. Figures 4a and 4b display the

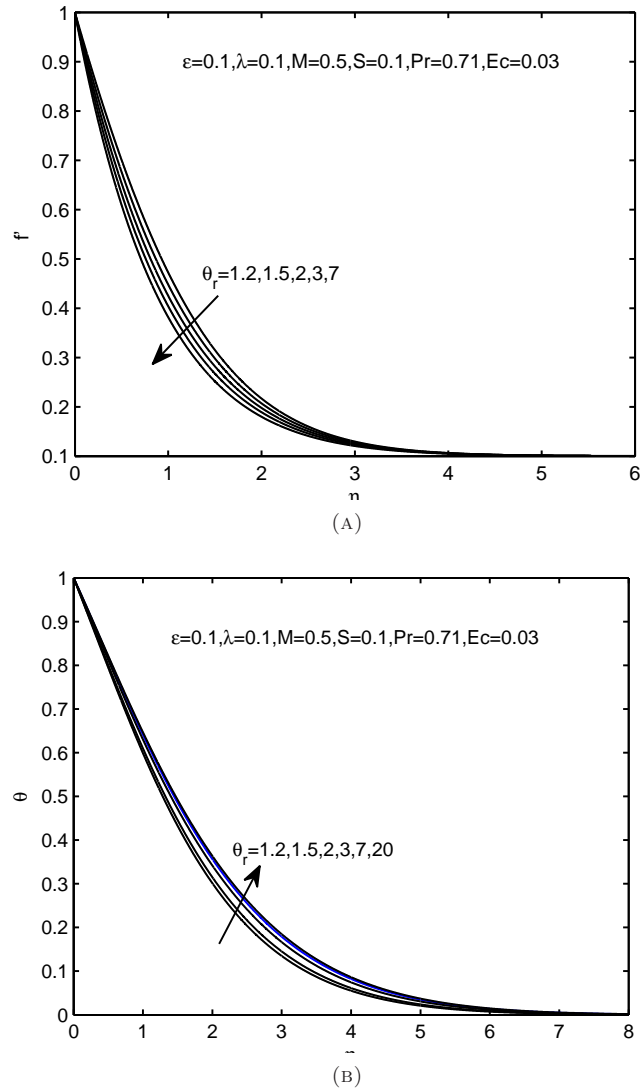


FIGURE 7. velocity and temperature profiles for different values of variable viscosity parameter θ_r

velocity and the temperature distributions for different values of the heat generation parameter S . It is seen from Figure 4a that the velocity profiles is influenced considerably and increases when the value of heat generation parameter increases. It is evident from Figure 4b the value of heat generation parameter increases, the temperature distribution also increases along the boundary. The influences of Eckert number on the dimensionless velocity and temperature functions are shown

in Figures 5a and 5b respectively. The Eckert number designates the ratio of the kinetic energy of the flow to the boundary layer enthalpy differences. It embodies the conversion of the kinetic energy into internal energy by work done against the viscous fluid stresses. The positive Eckert number implies cooling of the plate i.e., loss of heat from the plate to the fluid. Hence, greater viscous dissipative heat causes a rise in the temperature as well as the velocity. It is also evident from figures that the viscous dissipative effect is more in temperature and less in velocity field. For different values of the Prandtl number Pr , the velocity and the temperature profiles are plotted in Figures 6a and 6b respectively. The Prandtl number defines the ratio of momentum diffusivity to the thermal diffusivity. From Figure 6a, it is clear that an increase in the Prandtl number leads to a fall in the velocity. From Figure 6b, it is observed that an increase in the Prandtl number results a decrease of the thermal boundary layer thickness and in general lower average temperature within the boundary layer.

The reason is that smaller values of Pr are equivalent to increasing the thermal conductivities, and therefore heat is able to diffuse away from the heated surface more rapidly than for higher values of Pr . Hence in the case of smaller Prandtl numbers as the boundary layer is thicker and the rate of heat transfer is reduced. Effects of Viscosity parameter θ_r on the velocity and temperature profiles are clearly exhibited in Figures 7a and 7b respectively. Fluid velocity decreases with increasing values of viscosity parameter is noticed from the Figure 7a. It is observed from Figure 7b that the temperature profiles increases with increase of variable viscosity. This is due to the fact that increasing the variable viscosity parameter leads to increase in the skin-friction coefficient which causes a decrease in the velocity of the fluid. Physically, the thermal viscosity cause a rise in friction, when friction increases, the area of the stretching surface in contact with the flow increases, therefore generated heat from the friction on the surface is transferred to the flow. This leads to arise in the surface temperature and the flow is heated.

5. Conclusion

In this paper, we have studied the scaling group analysis of MHD effects on heat transfer near stagnation-point on a linearly stretching sheet with variable viscosity and thermal conductivity, viscous dissipation and heat source/sink. The viscosity of the fluid is assumed to be an inverse linear function of temperature and the thermal conductivity is assumed to vary linearly with temperature. The stretching velocity and surface temperature are assumed to vary linearly with distance from the stagnation point. The governing equations for the problem were changed to dimensionless non-linear ordinary differential equations using a scaling group of transformations. The scaling symmetry group is very essential procedure to comprehend the mathematical model and to find the similarity solutions for such type of flow which have wider applications in the engineering disciplines related to fluid mechanics. The transformed governing equations in the present study were solved numerically by using the Runge-Kutta fourth order along with shooting methods. The numerical results obtained agree very well with previously published data for

some particular cases of the present study. From the present study the following conclusions can be drawn:

- The magnetic field effects is to decelerate the velocity profiles whereas it increases the temperature profiles
- The effects of variable thermal conductivity parameter and heat source/sink parameters leads to increase in both temperature profiles and velocity profiles.
- Fluid velocity decreases with increasing values of variable viscosity parameter and it increases the temperature.
- Increasing the velocity ratio parameter tends to increase the velocity but decrease the temperature profiles.

References

1. L. J. Crane, *Flow past a stretching plate*, Z. Angew. Math. Phys. **21** (1970), 645–647.
2. K. B. Pavlov, *Magneto hydrodynamic flow of an incompressible viscous fluid caused by the deformation of a plane surface*, Magn. Gidrod. **10** (1974), 146–148.
3. P. S. Gupta, A. S. Gupta, *Heat and mass transfer on a stretching sheet with suction and blowing*, Can. J. Chem. Eng. **55** (1977), 744–746.
4. C. K. Chen, M. I. Char, *Heat transfer of a continuous stretching surface with suction or blowing*, J. Math. Anal. Appl. **135** (1988), 568–580.
5. I. Pop, T. Y. Na, *Unsteady flow past a stretching sheet*, Mech. Res. Commun. **23** (1996), 413–422.
6. K. Vajravelu, *Viscous flow over a nonlinearly stretching sheet*, Appl. Math. Comput. **124** (2001), 281–288.
7. R. Cortell, *Viscous flow and heat transfer over a nonlinearly stretching sheet*, Appl. Math. Comput. **184** (2007), 864–873.
8. L. Zheng, L. Wang, X. Zhang, *Analytic solutions of unsteady boundary flow and heat transfer on a permeable stretching sheet with non-uniform heat source/sink*, Commun. Nonlinear Sci. Numer. Simulat. **16** (2011), 731–740.
9. K. Bhattacharyya, *Effects of radiation and heat source/sink on unsteady MHD boundary layer flow and heat transfer over a shrinking sheet with suction/injection*, Front. Chem. Sci. Eng. **5** (2011), 376–384.
10. M. A. A. Mahmoud, S. E. Waheed, *MHD flow and heat transfer of a micro polar fluid over a stretching surface with heat generation (absorption) and slip velocity*, J. Egypt. Math. Soc. (2012), doi.org/10.1016/j.joems.2011.12.009.
11. K. Hiemenz, *Die Grenzschicht an einem in den gleichförmigen Flüssigkeitsstrom eingetauchten geraden Kreiszylinder*, Dingl. Polytech. J. **326** (1911), 321–326.
12. N. Ramachandran, T. Chen, T. Cebeci, P. Bradshaw, *Physical and Computational Aspects of Convective Heat Transfer*, Springer, New York, 1984.
13. K. Vajravelu, A. Hadjinicolaou, *Convective heat transfer in an electrically conducting fluid at a stretching surface with uniform free stream*, Internat. J. Engrg. Sci. **35** (1997), 1237–1244.
14. K. Hiemenz *Die Grenzschicht an einem in den gleichformigen Flüssigkeits-strom eingetauchten graden Kreiszylinder*. Dingler's, Poly. J. **326** (1911), 321–324.
15. T. C. Chiam, *Stagnation-point flow towards a stretching plate*. J. Phys. Soc. Jpn. **63** (1994), 2443–2444.
16. T. R. Mahapatra, A. S. Gupta, *Magnetohydrodynamic stagnation-point flow towards a stretching sheet*, Acta Mech. **152** (2001), 191–196.
17. P. M. Kishore, V. Rajesh, S. Vijayakumar, *The effects of thermal radiation and viscous dissipation on MHD heat and mass diffusion flow past on oscillating vertical plate embedded in a porous medium with variable surface conditions*, Theoret. Appl. Mech. **39** (2012), 90–125.

18. T. R. Mahapatra, A. S. Gupta, *Heat transfer in stagnation-point flow towards a stretching sheet*, Heat Mass Transfer. **38** (2002), 517–521.
19. R. Nazar, N. Amin, D. Filip, I. Pop, *Stagnation point flow of a micro polar fluid towards a stretching sheet*, Int. J. Nonlinear Mech. **39** (2004), 1227–1235.
20. G. C. Layek, S. Mukhopadhyay, Sk. A. Samad, *Heat and mass transfer analysis for boundary layer stagnation-point flow towards a heated porous stretching sheet with heat absorption/generation and suction/blowing*, Int. Commun. Heat Mass Transfer. **34** (2007), 347–356.
21. J. Zhu, L. Zheng, Z. G. Zhang, *Effects of slip condition on MHD stagnation-point flow over a power-law stretching sheet*, Appl. Math. Mech. **31** (2010), 439–448.
22. K. Bhattacharyya, G. C. Layek, *Effects of suction/blowing on steady boundary layer stagnation-point flow and heat transfer towards a shrinking sheet with thermal radiation*, Int. J. Heat Mass Transfer. **54** (2010), 302–307.
23. K. Bhattacharyya, S. Mukhopadhyay, G. C. Layek, *Slip effects on boundary layer stagnation-point flow and heat transfer towards a shrinking sheet*, Int. J. Heat Mass Transfer. **54** (2010), 307–313.
24. ———, *Slip effects on an unsteady boundary layer stagnation-point flow and heat transfer towards a stretching sheet*, Chin. Phys. Lett. **28** (2011), 694–702.
25. K. Bhattacharyya, *Dual solutions in boundary layer stagnation point flow and mass transfer with chemical reaction past a stretching/shrinking sheet*, Int. Commun. Heat Mass Transfer. **38** (2011), 917–922.
26. ———, *Dual solutions in unsteady stagnation-point flow over a shrinking sheet*, Chin. Phys. Lett. **28** (2011), 847.
27. A. J. Chamkha, Int. J. Eng. Sci. **42** (2004), 217.
28. I. Pop, R. S. R. Gorla, M. Rashidi, *The effect of variable viscosity on flow and heat transfer to a continuous moving flat plate*, Int. J. Eng. Sci. **30** (1992), 1–6 .
29. S. Mukhopadhyay, G. C. Layek, Sk. A. Samad, *Study of MHD boundary layer flow over a heated stretching sheet with variable viscosity*, Int. J. Heat Mass Transfer. **48** (2005), 4460–4466.
30. M. E. Ali, *The effect of variable viscosity on mixed convection heat transfer along a vertical moving surface*, Int. J. Therm. Sci. **45** (2006), 60–69.
31. M. Abd El-Aziz, *Temperature dependent viscosity and thermal conductivity effects on combined heat and mass transfer in MHD three-dimensional flow over a stretching surface with Ohmic heating*, Meccanica **42** (2007), 375–386.
32. Mohaimin, Ramasay Kandasamy, I. Hashim, *Variable viscosity and thermophoresis effects on Darcy mixed convective heat and mass transfer past a porous wedge in the presence of chemical reaction*, Theoret. Appl. Mech. **36** (2009), 29–46.
33. A. M. Salem, *Variable viscosity and thermal conductivity effects on MHD flow and heat transfer in viscoelastic fluid over a stretching sheet* Phys. Lett. A **369**(4) (2007), 315–322.
34. L. A. Hassanian, T. H. Al-arabi, *Non-Darcy unsteady mixed convection flow near the stagnation point on a heated vertical surface embedded in a porous medium with thermal radiation and variable viscosity*, Commun. Nonlinear Sci. Numer. Simulat. **14**(4) (2009), 1366–1376.
35. S. Sharidan, T. Mahmood, I. Pop, *Similarity solution for the unsteady boundary layer flow and heat transfer due to a stretching sheet* Int. J. Appl. Mech. Eng. **11** (2006), 647–654.
36. I. Pop, T. Y. Na, *Unsteady flow past a stretching sheet* Mech. Res. Commun. **23** (1996), 413–422.
37. R. N. Nazar, N. Amin, D. Filip, I. Pop, *Unsteady boundary layer flow in the region of the Stagnation-point on a stretching sheet*, Int. J. Eng. Sci. **42** (2004), 1241–1253.
38. M. A. Seddeek, F. A. Salama, *The effects of temperature dependent viscosity and thermal conductivity on unsteady MHD convective heat transfer past a semi-infinite vertical porous moving plate with variable suction*, Comp. Mater. Sci. **40** (2007), 186–192.
39. S. N. Odda, A. M. Farhan, *Chebyshev finite difference method for the effects of variable viscosity and variable thermal conductivity on heat transfer to a micro-polar fluid from a*

- non-isothermal stretching sheet with suction and blowing*. *Chaos Soliton. Fract.* **30** (2006), 851–858.
40. M. Shanmuga, *Effects of MHD and thermal radiation on forced convective flow over a power plate embedded in porous medium*, *Int. J. Theor. Appl. Mech.* **9** (2014), 1–4.
 41. B. I. Olajuwon, *Heat transfer in power law with variable thermal conductivity*, *Int. J. Theor. Appl. Mech.* **1** (2006), 13–20.
 42. M. A. Hossain, M. S. Munir, D. A. S. Rees, *Flow of viscous incompressible fluid with temperature dependent viscosity and thermal conductivity past a permeable wedge with uniform surface heat flux*, *Int. J. Therm. Sci.* **39** (2000), 635–644.
 43. Y. Z. Boutros, M. B. Abd-el-Malek, N. A. Badran, H. S. Hassan, *Lie-group method of solution for steady two dimensional boundary layer stagnation-point flow towards a heated stretching sheet placed in a porous medium*, *Meccanica* **41** (2006), 681–691.
 44. J. X. Ling, A. Dybbs, *Forced Convection over a flat plate submersed in a porous media: variable viscosity case*, ASME Winter Annual Meeting, Boston (1987), 13–18.
 45. F. C. Lai, F. A. Kulacki, *The effect of variable viscosity on convective heat transfer along a vertical surface in a saturated porous medium*, *Int. J. Heat Mass Transfer* **33** (1999), 1028–1033.
 46. H. Dessie, N. Kishan, *MHD effects on heat transfer over stretching sheet embedded in porous medium with variable viscosity, viscous dissipation and heat source/sink*, *Ain Shams Eng. J.* **5** (2014), 967–977.

**ГРУПНА СКАЛИРАНА АНАЛИЗА ЗА МХД ЕФЕКТЕ НА
ПРЕНОС ТОПЛОТЕ У БЛИЗИНИ ТАЧКЕ СТАГНАЦИЈЕ
УСЛЕД ЛИНЕАРНОГ ИСТЕЗАЊЕ ТАНКОГ СЛОЈА СА
ПРОМЕНЉИВОМ ВИСКОЗНОШЋУ И ТОПЛОТНОМ
ПРОВОДЉИВОШЋУ, ВИСКОЗНА ДИСИПАЦИЈА И
ТОПЛОТНИ ИЗВОР/ПОНОР**

РЕЗИМЕ. Анализирани су ефекти променљиве вискозности и топлотне проводљивости за МХД пренос топлоте тока вискозног нестишљивог електрично проводног флуида у близини тачке стагнације тока на непроводни истегљиви танки слој у присуству униформног магнетног поља са топлотним извором/понором. Парцијалне диференцијалне једначине кретања су сведене на обичне диференцијалне једначине користећи посебан облик Лијевих група трансформација, а затим решене помоћу методе Рунге–Кута четвртог реда. Анализирани су ефекти различитих физичких параметара на ток и карактеристике преноса топлоте. Варијације различитих параметара на коефицијент површинског трења - $f''(0)$ и температурни градијент $\theta'(0)$ представљени су у облику табеле.

Department of Mathematics
Osmania University
Hyderabad
India
hunegnawd@yahoo.com

(Received 22.03.2014)
(Revised 10.07.2015)

Department of Mathematics
Osmania University
Hyderabad
India
kishan_n@rediffmail.com